nature cell biology

LETTERS

Metabolic differentiation in the embryonic retina

Michalis Agathocleous[1,2,4], Nicola K. Love[1], Owen Randlett[1,4], Julia J. Harris[3], Jinyue Liu[1], Andrew J. Murray[1] and William A. Harris[1,5]

Unlike healthy adult tissues, cancers produce energy mainly by aerobic glycolysis instead of oxidative phosphorylation[1]. This adaptation, called the Warburg effect, may be a feature of all dividing cells, both normal and cancerous[2], or it may be specific to cancers[3]. It is not known whether, in a normally growing tissue during development, proliferating and postmitotic cells produce energy in fundamentally different ways. Here we show in the embryonic *Xenopus* retina *in vivo*, that dividing progenitor cells depend less on oxidative phosphorylation for ATP production than non-dividing differentiated cells, and instead use glycogen to fuel aerobic glycolysis. The transition from glycolysis to oxidative phosphorylation is connected to the cell differentiation process. Glycolysis is indispensable for progenitor proliferation and biosynthesis, even when it is not used for ATP production. These results suggest that the Warburg effect can be a feature of normal proliferation *in vivo*, and that the regulation of glycolysis and oxidative phosphorylation is critical for normal development.

We investigated the metabolic properties of a growing embryonic tissue, the retina of the frog *Xenopus laevis*, whose cells contain their own nutrient supply[4], allowing metabolic measurements of cells feeding on their intrinsic physiological nutrients. Retinal cells are all proliferative until stage 25, when differentiation begins, and by stage 41 cell cycle exit in the central retina is complete[5]. To determine whether proliferating and differentiated cells produce ATP in different ways, we inhibited oxidative phosphorylation by incubating embryos for 15 min with NaN_3, which inhibits Complex IV of the electron transport chain. ATP levels in the retina fell by 41% at stage 25, compared with 82% at stages 42–44 (Fig. 1a). The smaller drop in proliferating cells was not simply due to a slower ATP burn rate, because incubation with NaN_3 for 1 h did not further decrease ATP (Supplementary Fig. S1a). To determine whether this metabolic difference was intrinsic to retinal cells, we dissected retinae in modified Barth's solution (MBS), a salt buffer without nutrients. ATP levels in proliferating explants fell by significantly less than in differentiated explants after NaN_3 treatment (Fig. 1b and Supplementary Fig. S1b). Similar results followed inhibition of Complex III with antimycin A or of ATP synthase with oligomycin (Supplementary Fig. S1c,d). Differentiated cells might seem more oxidative because they rely more on external nutrients; however, in galactose-containing L15 medium or glucose-containing DMEM, ATP in differentiated but not proliferating explants was still severely depleted after NaN_3 treatment (Fig. 1c). Therefore, proliferating cells rely less on oxidative phosphorylation for ATP than differentiated cells *in vivo* or *ex vivo*, irrespectively of external nutrients. Proliferating cells from freshly explanted retinae consumed less O_2 in oxidative phosphorylation than differentiated cells (Fig. 1d). Intracellular lactate (Fig. 1e) and lactate dehydrogenase (LDH) activity (Fig. 1f) *in vivo* were elevated in proliferating when compared with differentiated cells, suggesting increased glycolysis.

A reduced dependence on oxidative phosphorylation might be peculiar to the embryonic *Xenopus* retina with its store of intracellular nutrients. To address this question, we looked at the embryonic zebrafish retina, where nutrients are delivered by the circulation. In these animals, differentiated cells in freshly explanted 78 h post-fertilization (hpf) retinae lost significantly more of their ATP after NaN_3 treatment than 26 hpf proliferating cells (Fig. 2a). We took advantage of the transparency of zebrafish embryos to image *in vivo* an energy-consuming process, microtubule polymerization, using Eb3–GFP (ref. 6), which moves with the plus end of polymerizing microtubules. After antimycin A treatment, retinal progenitors kept up Eb3 motion for significantly longer than differentiated neurons (Fig. 2b,c and Supplementary Movie). These results suggest that in the zebrafish retina, as in *Xenopus*, differentiated cells are more reliant on oxidative phosphorylation when compared with proliferating cells.

Proliferating cells in a stem cell niche might also depend less on oxidative phosphorylation. The frog retina continues to grow through life by the addition of cells from the ciliary margin[7]. Activity of succinate dehydrogenase (SDH), a citric acid cycle and electron transport chain

[1]Department of Physiology, Development and Neuroscience, University of Cambridge, Cambridge CB2 3DY, UK. [2]Gonville and Caius College, Cambridge CB2 1TA, UK. [3]Department of Neuroscience, Physiology and Pharmacology, University College London, London WC1E 6BT, UK. [4]Present addresses: Children's Research Institute, UT Southwestern, Dallas, Texas 75390, USA (M.A.); Department of Molecular and Cellular Biology, Harvard University, Cambridge, Massachusetts 02138, USA (O.R.). [5]Correspondence should be addressed to W.A.H. (e-mail: harris@mole.bio.cam.ac.uk)

Received 16 April 2012; accepted 24 May 2012; published online 1 July 2012; DOI: 10.1038/ncb2531

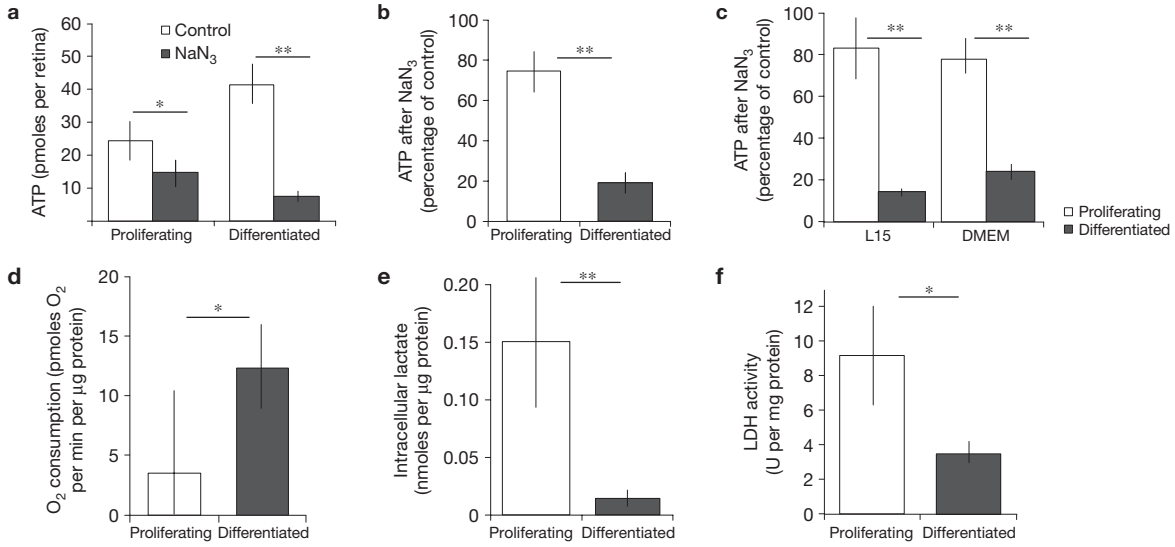

Figure 1 Proliferating cells rely less than differentiated cells on oxidative phosphorylation for ATP, and have higher levels of glycolysis. (**a**–**c**) ATP in proliferating or differentiated retinae after inhibition of oxidative phosphorylation with NaN_3: (**a**) for 15 min *in vivo*, showing ATP per retina (proliferating, $n=5$, $P=0.03$; differentiated, $n=5$, $P=5\times10^{-6}$); (**b**) for 10 min in explants in MBS, showing the percentage of ATP when compared with controls (proliferating, $n=13$, $P=0.002$; differentiated, $n=11$, $P=3\times10^{-5}$ compared with controls; proliferating–differentiated comparison, $P=4\times10^{-8}$); (**c**) and in explants in L15 (proliferating, $n=5$, $P=0.3$; differentiated, $n=5$, $P=0.0009$ compared with controls; proliferating–differentiated comparison, $P=4\times10^{-7}$) or DMEM (proliferating, $n=4$, $P=0.06$; differentiated, $n=5$, $P=5\times10^{-7}$ compared with controls; proliferating–differentiated comparison, $P=10^{-5}$). (**d**) Rate of oxygen consumption in fresh retinal explants in L15 ($n=6$, $P=0.03$). (**e**) Amount of intracellular lactate of proliferating and differentiated retinae *in vivo* (proliferating, $n=5$; differentiated, $n=7$; $P=10^{-4}$). (**f**) LDH activity of proliferating and differentiated retinae ($n=7$, $P=0.003$). All error bars show 95% confidence intervals; $^{*}0.001<P<0.05$; $^{**}P<0.001$.

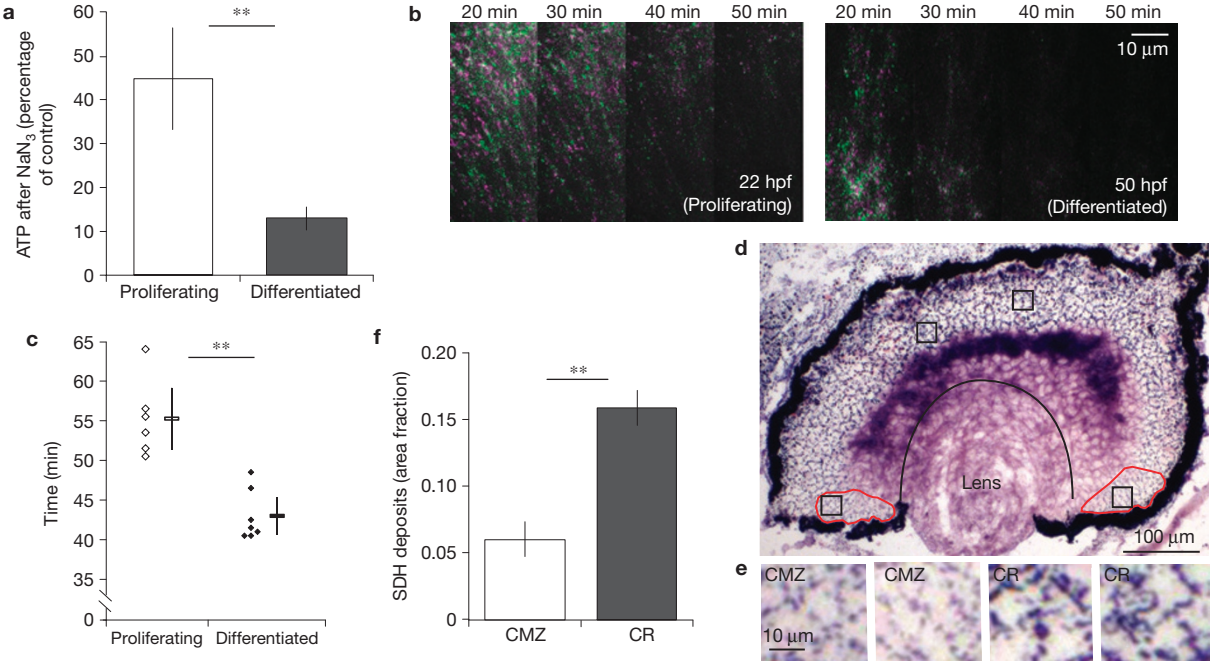

Figure 2 Metabolic differences between progenitors and differentiated cells are also present in the postembryonic retinal stem cell niche, and in the zebrafish retina. (**a**) ATP levels in freshly explanted zebrafish retinae in L15 after inhibition of oxidative phosphorylation with NaN_3 for 10 min (proliferating, $n=14$, $P=0.0002$; differentiated, $n=15$, $P=4\times10^{-8}$; proliferating–differentiated comparison, $P=8\times10^{-7}$). (**b**) Eb3–GFP imaging in the zebrafish retina. Each panel is the merged image of two frames 20 s apart, coloured green or magenta, at the indicated time after antimycin A treatment. Dots that moved between frames should be green or magenta. Proliferating cells (left) keep up Eb3–GFP motion for longer than differentiated cells (right). (**c**) Time taken after antimycin A treatment for the Eb3–GFP motion to stop in differentiated 50–54 hpf retinae ($n=7$ movies) and proliferating 22–26 hpf retinae ($n=6$). Averages are shown next to individual data points ($P=0.0002$). (**d**) Dark deposits as a result of SDH activity in a retinal section that includes proliferating ciliary margin zone cells (CMZ, circumscribed in red) and differentiated central retina cells (CR, region between the pigmented epithelium, lens and CMZ). (**e**) Magnification of the areas outlined by squares in **d**, showing that deposits in the CMZ are both fainter and less dense than in the central retina cells. (**f**) Quantification of the area fraction covered by deposits ($n=43$, $P<10^{-10}$). All error bars show 95% confidence intervals; $^{**}P<0.001$.

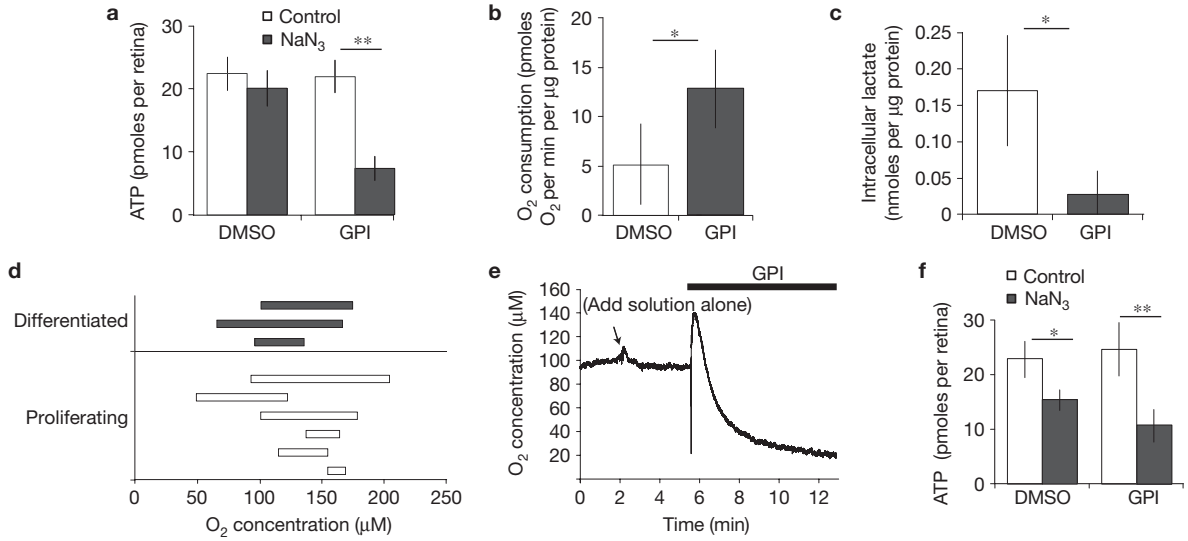

Figure 3 Inhibition of glycogen breakdown shifts energy production from glycolysis to oxidative phosphorylation. (**a**) ATP levels in freshly explanted proliferating retinae in MBS pre-incubated with GPI for 20 min, followed by 10 min of NaN_3 treatment (dimethylsulphoxide (DMSO), $n=22$, $P>0.05$; GPI, $n=27$, $P=5\times10^{-12}$). (**b**) Rate of oxygen consumption in fresh retinal explants incubated with GPI in L15 ($n=9$, $P<0.05$). (**c**) Intracellular lactate in retinal explants incubated for 3 h with GPI ($n=4$, $P=0.01$). (**d**) Each bar represents the range of O_2 concentrations sampled from various points in the retina of a live embryo at stage 25 (proliferating) or stage 41 (differentiated). (**e**) Addition of GPI in the medium while recording from a specific point in the proliferating retinae lowers O_2 concentration (4/4 experiments, decrease ranging from 8 to 73 µM O_2, depending on the depth sampled from the surface; no decrease observed with control solutions; the momentary upward spike is a response to adding more solution). (**f**) Inhibition of oxidative phosphorylation with NaN_3 at stage 25 *in vivo* reduced ATP in the retina to a greater extent in GPI-treated embryos (57% drop, $n=8$, $P=0.0004$) when compared with controls (33% drop, $n=9$, $P=0.005$). All error bars show 95% confidence intervals; $^{*}0.001<P<0.05$; $^{**}P<0.001$.

enzyme, often indicates oxidative activity, and is used to distinguish aerobic from glycolytic muscle fibres[8]. SDH activity was lower in the ciliary margin than in the differentiated central retina *in vivo* (Fig. 2d–f), consistent with the idea that dividing cells respire less than differentiated cells even when they are neighbours in the same tissue.

To determine whether proliferating cells produce ATP by glycolysis, stage 25 retinal explants were incubated with 2-deoxy-D-glucose (2DG), which inhibits glycolysis by blocking the ability of hexokinase to phosphorylate glucose to glucose-6-phosphate. 2DG, however, had no effect on ATP in the presence or absence of NaN_3, or on intracellular lactate (Supplementary Fig. S1e,f). We wondered, therefore, whether there was another entry into the glycolytic pathway in these embryonic *Xenopus* cells, which, for example, have abundant intracellular glycogen[9,10]. Glycogen is broken down to glucose-1-phosphate, which is converted to glucose-6-phosphate and enters glycolysis, bypassing hexokinase. Incubation of stage 25 retinae with a glycogen phosphorylase inhibitor[11] (GPI) did not affect ATP levels. However, ATP now became sensitive to NaN_3 (Fig. 3a). GPI-treated proliferating retinal explants used more oxygen in oxidative phosphorylation than controls (Fig. 3b), and produced less lactate (Fig. 3c). The addition of extracellular carbohydrate was insufficient to support non-oxidative ATP generation in the presence of GPI (Supplementary Fig. S1g). Access to glycogen stores is therefore required for aerobic glycolysis in these proliferating cells, and in its absence, they shift to oxidation of other endogenous substrates[4]. High glycogen levels have been reported in some cancers[12], and glycogen phosphorylase inhibition can reduce growth in cancer cell lines[13]. In conjunction with upregulated glucose transport, glycogen deposition may therefore also promote glycolysis in some proliferating cells that feed externally, similarly to its proposed function in astrocytes[14], particularly when the nutrient supply is developing or fluctuating.

Despite the ability of proliferating cells to become facultatively aerobic in explants, we wondered whether they might be obligatorily glycolytic *in vivo* because of a hypoxic environment compared with differentiated cells, as has been suggested for some adult stem cells[15]. We therefore recorded oxygen concentrations *in vivo* using an oxygen electrode. Oxygen levels were similar in proliferating and differentiated retinae (Fig. 3d). Incubation of embryos with GPI decreased local [O_2] in proliferating retinae (Fig. 3e), consistent with increased oxygen consumption[16], and retinae became more dependent on oxidative phosphorylation for ATP (Fig. 3f). Therefore, the glycolytic metabolism of progenitors in explants or *in vivo* is not due to restricted access to oxygen, or to impairment of the respiratory machinery, and is also not due to insufficiency of oxidative phosphorylation to serve energetic demands. Rather, it seems that these cells choose to be glycolytic.

To investigate whether metabolism is regulated by the cellular differentiation program, we forced progenitors to exit the cell cycle prematurely and to differentiate into the first-born retinal neurons, retinal ganglion cells. Xath5GR, an inducible version of the transcription factor Xath5 (ref. 17), was expressed by injection of RNA *in vivo* and activated by dexamethasone at the beginning of neurogenesis at stage 25. This led to rapid cell cycle exit and precocious isl1 expression, which marks retinal ganglion cells and other differentiated cells (Fig. 4a and Supplementary Fig. S2). Xath5GR-positive cells sorted from stage 37/8 retinae were more dependent on oxidative phosphorylation for ATP when compared with Xath5GR-negative cells from the same retinae (Fig. 4b,c). This indicates that the metabolic shift to oxidation can be influenced by the same transcription factors that control cell differentiation.

The metabolic switch after GPI treatment presented the opportunity to investigate the proposed role of the Warburg effect in proliferation

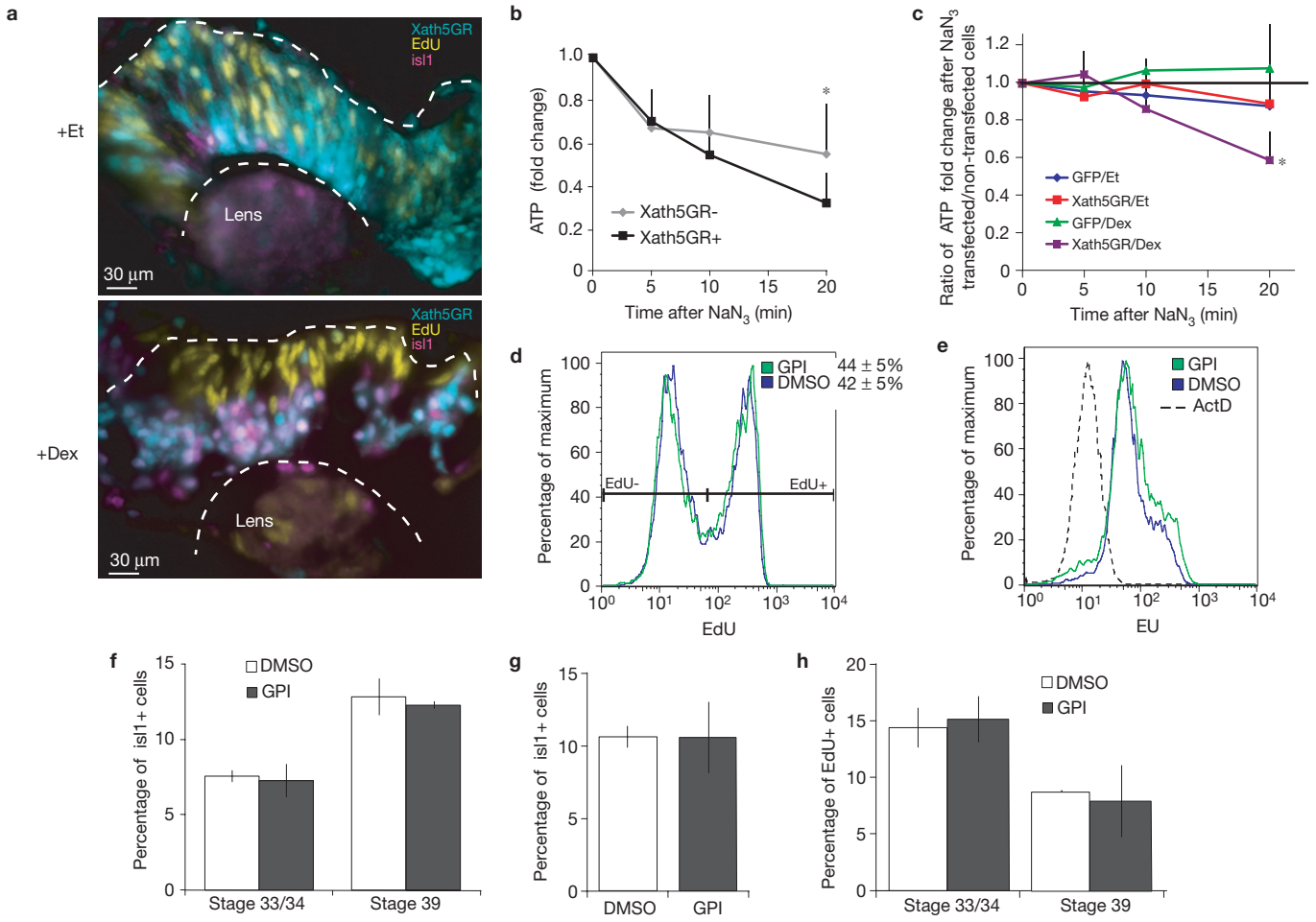

Figure 4 Cell differentiation can affect energy metabolism, whereas shifting energy metabolism to oxidative phosphorylation does not influence aspects of proliferation and differentiation. (**a**) Activation of Xath5GR (expressed in cyan cells) by dexamethasone (Dex; bottom panel) promotes cell cycle exit, migration to the basal layer where ganglion cells normally reside, and expression of isl1, compared with non-expressing cells in the same retina, or with Xath5GR-expressing cells receiving ethanol solvent (Et; top panel). (**b**) Sorted Xath5GR-positive cells lose ATP faster after NaN_3 addition when compared with Xath5GR-negative cells in the same retina ($n=4$, $P<0.05$ at $t=20$). (**c**) The ratio of ATP remaining after NaN_3 treatment in construct-expressing/non-expressing cells from the same retinae is <1 at $t=20$ in the Xath5GR + Dex condition and not when dexamethasone is omitted or when GFP messenger RNA is injected with or without dexamethasone ($n=4$, $P=0.04$). (**d**) GPI does not change the proportion of cells incorporating the nucleotide analogue EdU in DNA after a brief pulse, nor the amount of EdU per cell ($n=9$). (**e**) GPI treatment for 8–10 h in explants in MBS does not change the amount of the nucleotide analogue 5-ethynyl uridine (EU) incorporated into RNA ($n=6$). The dashed line shows the background fluorescence signal after inhibition of RNA synthesis with actinomycin D (ActD). Quantification is shown in Fig. 5h. (**f**) Incubation of stage 25 embryos for 1 or 2 days with GPI *in vivo* does not change the proportion of isl1+ differentiated cells present by stages 33/4 or 39 ($n=9$, $P>0.05$). (**g**) Incubation of stage 25 explants for 1 d with GPI in 1 × MBS does not change the proportion of isl1+ differentiated cells present by stage 35/6 ($n=4$, $P>0.05$). (**h**) Incubation of stage 25 embryos for 1 or 2 days with GPI *in vivo* does not change the proportion of cells that are labelled by a pulse of EdU and therefore have not exited the cell cycle by stages 33/4 or 39 ($n=5$, $P>0.05$). All error bars show 95% confidence intervals; $^*0.001<P<0.05$.

in our system. Surprisingly, treatment of stage 25 retinal explants for 5–10 h (Supplementary Fig. S3a) with GPI did not affect proliferation, or rates of RNA and protein synthesis (Fig. 4d,e and Supplementary Fig. S3b,c). Nor did the proportion of cells that exited the cell cycle and differentiated into isl1-positive cells change after 1 or 2 days of GPI treatment *in vivo* or in explants (Fig. 4f–h). These results suggest that the use of glycolysis for energy production may not be absolutely required for normal proliferation or aspects of differentiation in the progenitors.

As glycolysis through glycogen is not required for proliferation, perhaps cells may use other endogenous nutrients to run glycolysis when glycogen is cut off. We therefore blocked both glycolytic entry points with a combination of GPI and 2DG. Cells maintained their ATP (Fig. 5a), and lactate did not decrease further than with GPI alone (Fig. 5b). However, after 8–10 h of this complete block in explants in MBS, the rate of ethynyl deoxyuridine (EdU) incorporation diminished (Fig. 5c,d) and cells slowed down or arrested in S phase (Fig. 5e,f and Supplementary Fig. S3d) without overt changes in the proportion of new G1 cells entering S phase, or the proportion of G2/M cells that remained EdU negative after a short EdU pulse[18] (Supplementary Fig. S3e–g). These results suggest that the rate of S phase is compromised when glycolysis is blocked. We found that progenitors have high levels of RNA synthesis when compared with most differentiated cells (Fig. 5g), particularly in S/G2 (Supplementary Fig. S3h) and blocking glycolysis reduced RNA synthesis in S/G2 phase (Fig. 5h). Protein synthesis was reduced throughout the cell cycle (Fig. 5i,j) and

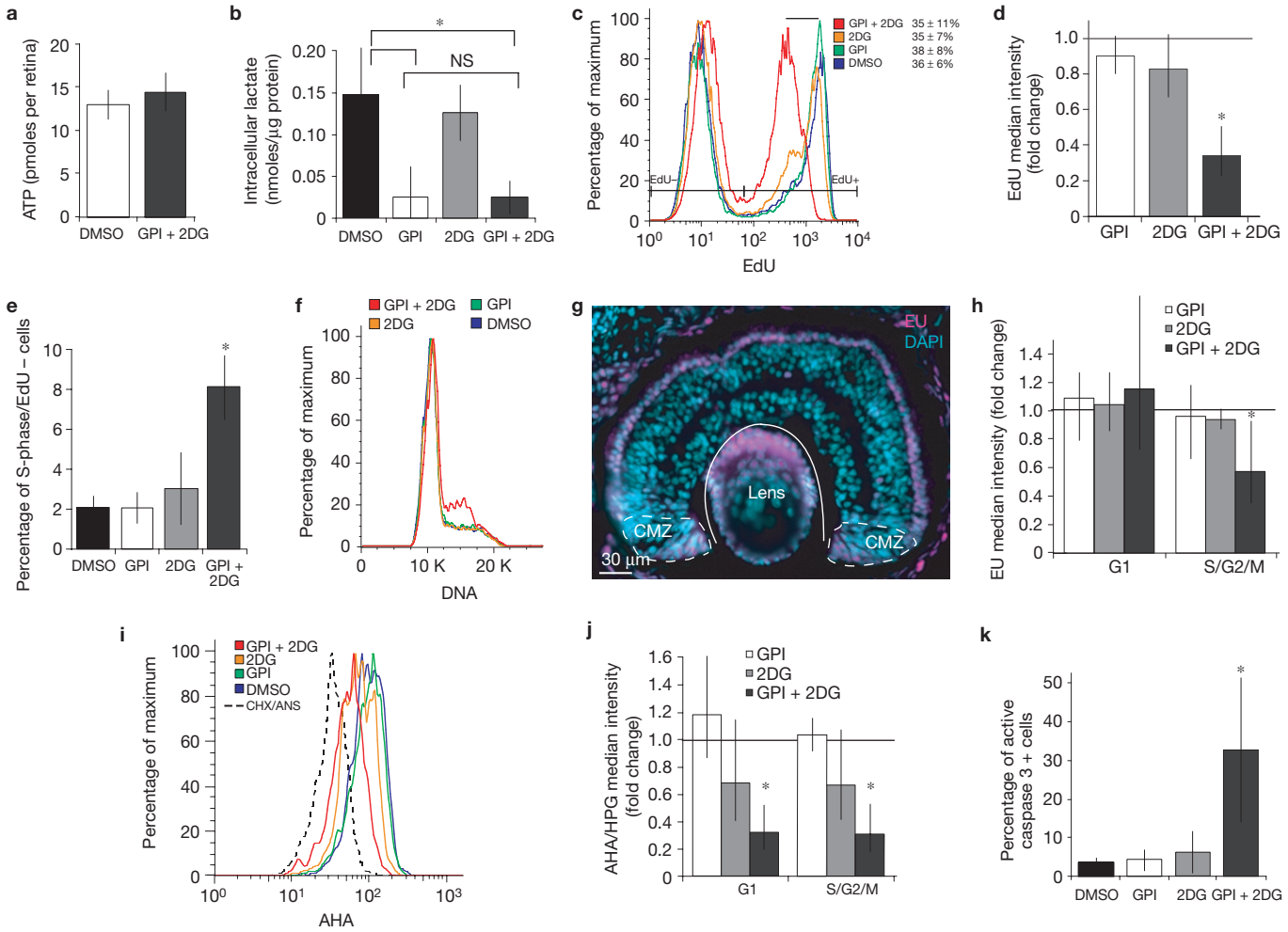

Figure 5 Complete glycolytic block inhibits progenitor proliferation, biosynthesis and survival. (**a**) ATP in explants in MBS does not change after 30 min of GPI + 2DG treatment ($n = 20$). (**b**) Intracellular lactate after 3 h of GPI and/or 2DG treatment (data from the same set of experiments as Fig. 3c and Supplementary Fig. S1f; GPI + 2DG, $n = 6$, $P = 0.003$ compared with control, $P > 0.05$ compared with GPI). (**c**–**f**) GPI + 2DG but neither drug alone, for 8–10 h in MBS in explants: (**c**,**d**) reduces EdU incorporation per cell after a short pulse ($n = 4$, $P = 0.006$) (black bar indicates shift in histogram) but not the percentage of EdU+ cells; (**e**) increases the proportion of S phase cells that do not incorporate EdU ($n = 3$, $P = 0.02$); (**f**) causes cells to accumulate in S phase (observed in 10/11 experiments for GPI + 2DG; 3/13 for GPI and 1/11 for 2DG). (**g**) The nucleotide analogue 5-ethynyl-uridine (EU) is incorporated in RNA at much higher levels in CMZ proliferating cells and in photoreceptors when compared with other retinal differentiated cells *in vivo* (stage 41). (**h**–**k**) GPI + 2DG but not either drug alone: (**h**) reduces incorporation of EU into RNA in S/G2 ($n = 4$, $P = 0.03$); (**i**,**j**) reduces incorporation of the methionine analogues AHA or HPG into proteins in G1 ($n = 4$, $P = 0.02$) and S/G2 ($n = 4$, $P = 0.02$; dashed line is the background fluorescence signal when the protein synthesis inhibitors cycloheximide + anisomycin are used with AHA); (**k**) increases the proportion of active-caspase-3 + apoptotic cells ($n = 5$, $P = 0.03$). All error bars show 95% confidence intervals; $^*0.001 < P < 0.05$; NS, not significant.

progenitors went into apoptosis (Fig. 5k). Therefore, some amount of glycolysis is required for normal rates of proliferation, RNA and protein synthesis and survival of retinal progenitors, even if energy levels can be maintained by oxidative phosphorylation.

Previous work found proliferating lymphocytes[19] and thymocytes[20] to be glycolytic, whereas embryonic stem cells showed either increased[21] or decreased oxidative phosphorylation when compared with more differentiated cells[22,23]. A major limitation of these studies of cultured cells is that metabolism *in vitro* may depend on the experimentally defined nutrient or oxygen conditions[24]. Our results argue that the Warburg effect can be a feature of physiological cell proliferation *in vivo*, and that it is connected to the differentiation process. We find that using glycolysis for energy may not be the only way to promote high biosynthesis, and speculate that when forced to turn to oxidative phosphorylation for energy, cells may operate gluconeogenic–glycolytic cycles, starting from their abundant intracellular protein and lipid stores[4], to sustain high glycolytic rates. Furthermore, carbohydrate from glycosylated protein stores, including mannose, galactose and glucosamine[25], could be an alternative source for glycolysis. *Xenopus* retinal progenitors required glycolysis even when they did not use it for energy, indicating that, unlike some other cells, they cannot substitute glycolysis with alternative pathways such as glutaminolysis[26]. In yeast[27] and mammalian cell lines[28], energy metabolism varies with cell cycle phase, and it will be interesting to examine the connections between energy metabolism and cell cycle progression in development. Previously reported changes in metabolic enzyme expression[29], reactive oxygen species[30] and other aspects of energy metabolism[31] during differentiation indicate that regulation of the core metabolic strategies we report here is likely to play a role in diverse developmental contexts. □

METHODS

Methods and any associated references are available in the online version of the paper.

Note: Supplementary Information is available in the online version of the paper

ACKNOWLEDGEMENTS

We are grateful to F. Gallagher and H. Sladen for help with the LDH assays, N. Miller for cell sorting and D. Attwell for advice on the oxygen concentration measurements. We thank J. Bixby, C. Holt, S. Morrison, S. He and R. Johnson for comments on the manuscript. We thank the Wellcome Trust (W.A.H.) and Gonville and Caius College and the Royal Commission for the Exhibition of 1851 (M.A.) for financial support.

AUTHOR CONTRIBUTIONS

M.A. conceived the study, carried out most of the experiments and co-wrote the paper. N.K.L. did the LDH and lactate assays and helped with several other aspects of the experimental work. O.R. did the Eb3–GFP imaging in zebrafish. J.J.H. did the *in vivo* oxygen recordings. J.L. did the SDH histochemistry. The oxygen consumption assays were done with A.J.M. W.A.H. guided the research and co-wrote the paper.

COMPETING FINANCIAL INTERESTS

The authors declare no competing financial interests.

Published online at www.nature.com/doifinder/10.1038/ncb2531
Reprints and permissions information is available online at www.nature.com/reprints

1. Warburg, O. On the origin of cancer cells. *Science* **123,** 309–314 (1956).
2. Vander Heiden, M. G., Cantley, L. C. & Thompson, C. B. Understanding the Warburg effect: the metabolic requirements of cell proliferation. *Science* **324,** 1029–1033 (2009).
3. Gatenby, R. A. & Gillies, R. J. Why do cancers have high aerobic glycolysis? *Nat. Rev. Cancer* **4,** 891–899 (2004).
4. Jorgensen, P., Steen, J. A. J., Steen, H. & Kirschner, M. W. The mechanism and pattern of yolk consumption provide insight into embryonic nutrition in Xenopus. *Development* **136,** 1539–1548 (2009).
5. Holt, C. E., Bertsch, T. W., Ellis, H. M. & Harris, W. A. Cellular determination in the Xenopus retina is independent of lineage and birth date. *Neuron* **1,** 15–26 (1988).
6. Norden, C., Young, S., Link, B. A. & Harris, W. A. Actomyosin is the main driver of interkinetic nuclear migration in the retina. *Cell* **138,** 1195–1208 (2009).
7. Agathocleous, M. & Harris, W. A. From progenitors to differentiated cells in the vertebrate retina. *Annu. Rev. Cell Dev. Biol.* **25,** 45–69 (2009).
8. Burke, R. E., Levine, D. N. & Zajac, F. E. 3rd Mammalian motor units: physiological-histochemical correlation in three types in cat gastrocnemius. *Science* **174,** 709–712 (1971).
9. Perry, M. M. Identification of glycogen in thin sections of amphibian embryos. *J. Cell Sci.* **2,** 257–264 (1967).
10. Rodriguez, I. R. & Fliesler, S. J. Glycogenesis in the amphibian retina: *in vitro* conversion of [2-3H] mannose to [3H] glucose and subsequent incorporation into glycogen. *Exp. Eye Res.* **51,** 71–77 (1990).
11. Klabunde, T. *et al.* Acyl ureas as human liver glycogen phosphorylase inhibitors for the treatment of type 2 diabetes. *J. Med. Chem.* **48,** 6178–6193 (2005).
12. Takahashi, S. *et al.* Estimation of glycogen levels in human colorectal cancer tissue: relationship with cell cycle and tumour outgrowth. *J. Gastroenterol.* **34,** 474–480 (1999).
13. Schnier, J. B., Nishi, K., Monks, A., Gorin, F. A. & Bradbury, E. M. Inhibition of glycogen phosphorylase (GP) by CP-91,149 induces growth inhibition correlating with brain GP expression. *Biochem. Biophys. Res. Commun.* **309,** 126–134 (2003).
14. Pellerin, L. & Magistretti, P. J. Sweet sixteen for ANLS. *J. Cereb. Blood Flow Metab.* http://dx.doi.org/10.1038/jcbfm.2011.149 (2011).
15. Nakada, D., Levi, B. P. & Morrison, S. J. Integrating physiological regulation with stem cell and tissue homeostasis. *Neuron* **70,** 703–718 (2011).
16. Hall, C. N. & Attwell, D. Assessing the physiological concentration and targets of nitric oxide in brain tissue. *J. Physiol.* **586,** 3597–3615 (2008).
17. Hutcheson, D. A. & Vetter, M. L. The bHLH factors Xath5 and XNeuroD can upregulate the expression of XBrn3d, a POU-homeodomain transcription factor. *Dev. Biol.* **232,** 327–338 (2001).
18. Locker, M. *et al.* Hedgehog signalling and the retina: insights into the mechanisms controlling the proliferative properties of neural precursors. *Genes Dev.* **20,** 3036–3048 (2006).
19. Wang, T., Marquardt, C. & Foker, J. Aerobic glycolysis during lymphocyte proliferation. *Nature* **261,** 702–705 (1976).
20. Brand, K. & Hermfisse, U. Aerobic glycolysis by proliferating cells: a protective strategy against reactive oxygen species. *FASEB J.* **11,** 388–395 (1997).
21. Birket, M. J. *et al.* A reduction in ATP demand and mitochondrial activity with neural differentiation of human embryonic stem cells. *J. Cell Sci.* **124,** 348–358 (2011).
22. Chung, S. *et al.* Mitochondrial oxidative metabolism is required for the cardiac differentiation of stem cells. *Nat. Clin. Pract. Cardiovasc. Med.* **4,** S60–S67 (2007).
23. Facucho-Oliveira, J. M. & St John, J. C. The relationship between pluripotency and mitochondrial DNA proliferation during early embryo development and embryonic stem cell differentiation. *Stem Cell Rev. Rep.* **5,** 140–158 (2009).
24. Cairns, R. A., Harris, I. S. & Mak, T. W. Regulation of cancer cell metabolism. *Nat. Rev. Cancer* **11,** 85–95 (2011).
25. Gottlieb, T. A. & Wallace, R. A. Intracellular glycosylation of vitellogenin in the liver of estrogen-stimulated Xenopus laevis. *J. Biol. Chem.* **257,** 95–103 (1982).
26. Yang, C. *et al.* Glioblastoma cells require glutamate dehydrogenase to survive impairments of glucose metabolism or Akt signalling. *Cancer Res.* **69,** 7986–7993 (2009).
27. Tu, B. P., Kudlicki, A., Rowicka, M. & McKnight, S. L. Logic of the yeast metabolic cycle: temporal compartmentalization of cellular processes. *Science* **310,** 1152–1158 (2005).
28. Almeida, A., Bolanos, J. P. & Moncada, S. E3 ubiquitin ligase APC/C-Cdh1 accounts for the Warburg effect by linking glycolysis to cell proliferation. *Proc. Natl Acad. Sci. USA* **107,** 738–741 (2010).
29. Ozbudak, E. M., Tassy, O. & Pourquie, O. Spatiotemporal compartmentalization of key physiological processes during muscle precursor differentiation. *Proc. Natl Acad. Sci. USA* **107,** 4224–4229 (2010).
30. Owusu-Ansah, E. & Banerjee, U. Reactive oxygen species prime *Drosophila* haematopoietic progenitors for differentiation. *Nature* **461,** 537–541 (2009).
31. Lopaschuk, G. D. & Jaswal, J. S. Energy metabolic phenotype of the cardiomyocyte during development, differentiation, and postnatal maturation. *J. Cardiovasc. Pharmacol.* **56,** 130–140 (2010).

METHODS

ATP assays. For *in vivo* measurements, drugs were added to the embryo medium, retinae were dissected into 1% perchloric acid and ATP was measured using the ATP bioluminescence kit CLS II (Roche). For measurements in explants, retinae were dissected in 1 × MBS, L15 or DMEM (Invitrogen) and drugs were immediately added for the duration indicated in the text.

Oxygen consumption. Retinae were dissected in either 1 × MBS or L15 and oxygen consumption was immediately measured using Clark-type oxygen electrodes with fast-responding FEP membranes in respiration chambers (Strathkelvin Instruments). The rate of oxygen consumption due to oxidative phosphorylation was the difference before and after 5 μM antimycin + 4 mM NaN_3 treatment. Soluble protein content for normalization was measured using the BCA assay kit (Thermo Scientific).

LDH activity. Freshly dissected retinae of stage 25–28 and stage 44–45 embryos were sonicated in 0.1 × MBS. Tris buffer (48 mM, pH 7.4), NADH (0.4 mM, Sigma) and sodium pyruvate (0.9 mM, Sigma) were added, and the rate of NADH consumption was measured[32]. Total soluble protein for normalization was extracted using the same procedure.

Lactate assays. Dissected retinae were immediately frozen on dry ice, and intracellular lactate was extracted by sonication in 1 × MBS and measured using a Fluorometric Lactate assay kit (Abcam) in accordance with the manufacturer's instructions. Lactate values were normalized to soluble protein content. For drug tests, fresh retinal explants were incubated at room temperature with 2DG or GPI for 3 h before analysis.

Eb3–GFP imaging. Embryos were injected with Eb3–GFP mRNA (ref. 6), and grown until 22–26 hpf or 50–54 hpf. Embryos from both stages were mounted on the same dish and imaged simultaneously by spinning-disc confocal microscopy every 20 s.

SDH histochemistry. Fresh unfixed cryostat sections were incubated at room temperature for 2 h with 50 mM sodium succinate, 1 mM 1-methoxy phenazine methosulphate, 0.5 mM sodium azide and 1.3 mM nitroblue tetrazolium in 100 mM phosphate buffer (all from Sigma). Oxidation of succinate by the endogenous SDH reduces nitroblue tetrazolium to give a dark cytoplasmic stain. Omission of succinate from the mixture resulted in negligible staining, showing that the staining was due to specific SDH activity (data not shown). The fraction of the retinal area covered by the deposits was measured automatically using CellProfiler[33].

$[O_2]$ measurements *in vivo*. $[O_2]$ was measured using a probe with a tip <10 μm (Unisense), which was calibrated by immersion in N_2-bubbled water, containing negligible O_2, and air-equilibrated water, containing 210 μM O_2 (ref. 16). Experiments were performed in a chamber containing 1 × MBS and drugs were added directly to the chamber during the recording period. The embryo was immobilised under a harp, with one eye (skin removed) facing upwards. The O_2 probe was lowered directly into the eye in a stepwise fashion, to maximum depths of 200 μm. Stepping deeper in the retina incrementally lowered the recorded $[O_2]$ (Supplementary Fig. S4a). Adding NaN_3 rapidly increased local $[O_2]$, showing that O_2 consumption during respiration is responsible for lowering $[O_2]$ inside the embryo (Supplementary Fig. S4b).

Xath5GR experiments. Xath5GR mRNA (150 pg) was co-injected with 70 pg of GFP mRNA in the two dorsal blastomeres of the eight-cell-stage blastula, and 4 μg ml^{-1} dexamethasone was added at stage 25. Freshly dissected retinae were dissociated, cells on ice were sorted on the basis of GFP intensity into GFP+ and GFP− tubes in 1 × MBS + 0.5% BSA using a MoFlo (Dako), and each tube was split into four microplate wells, for time points $t = 0$, 5, 10, 20 min in the ATP/NaN_3 assay. For flow cytometric analysis, after *in vivo* dexamethasone induction at stage 25, retinae were dissected at the indicated stage and dissociated, fixed and stained for isl1. For EdU, explants were incubated for 1 h in EdU before fixation. For staining on sections, EdU was injected in the embryo for 1–2 h, and the embryo was fixed and sectioned.

Flow cytometry, DNA, RNA and protein synthesis assays. The following reagents (Click-iT assay kits, Invitrogen) were used on retinal explants in 1 × MBS, in the time immediately before dissociation and fixation: 0.5 mM EdU (DNA) for 1–2 h, 2–5 mM EU (RNA) for 2–5 h, and 1 mM AHA or HPG (protein) for 2–4 h. Cells were dissociated using trypsin digestion for 10 min, fixed in 2% formaldehyde for 30 min on ice, stained with antibodies (anti-active caspase 3 (1:300, rabbit, BD Biosciences, no. 559565), anti-GFP (1:500, rabbit, Molecular Probes, no. A-11122), anti-isl1 (1:100, mouse 40.2D6, DSHB)) and/or the Click-iT assay kits according to the manufacturer's instructions and with DAPI (1 μg ml^{-1}), and analysed on a CyAn-ADP (Dako). Results were analysed using FlowJo (TreeStar). To calculate fold changes in median fluorescent intensity (MFI) in EU or AHA/HPG incorporation, for each experiment the background MFI (when actinomycin D or cycloheximide + anisomycin were used to inhibit RNA and protein synthesis respectively) was deducted from the MFI of the other conditions. For *in vivo* DNA or RNA synthesis, EdU or EU was injected in embryos 2 h (EdU) or 5 h (EU) before fixation and embryos were fixed, cryosectioned, and slides stained using standard procedures.

Drugs. The drugs were as follows: 20 mM NaN_3 (Sigma); 36 μM antimycin A (Sigma); 25 μM GPI, 1-(3-(3-(2-chloro-4,5-difluorobenzoyl)ureido)-4-methoxyphenyl)-3-methylurea (Calbiochem); 20 mM 2DG (Sigma); 20 μM oligomycin (Sigma). In experiments with GPI *in vivo*, the skin in the anterior embryo was removed to allow drug penetration.

Statistics. Results were analysed with a two-tailed *t*-test and error bars shown are 95% confidence intervals.

32. Moran, J. H. & Schnellmann, R. G. A rapid beta-NADH-linked fluorescence assay for lactate dehydrogenase in cellular death. *J. Pharmacol. Toxicol. Methods* **36,** 41–44 (1996).
33. Carpenter, A. E. *et al.* CellProfiler: image analysis software for identifying and quantifying cell phenotypes. *Genome Biol.* **7,** R100 (2006).

DOI: 10.1038/ncb2531

nature cell biology

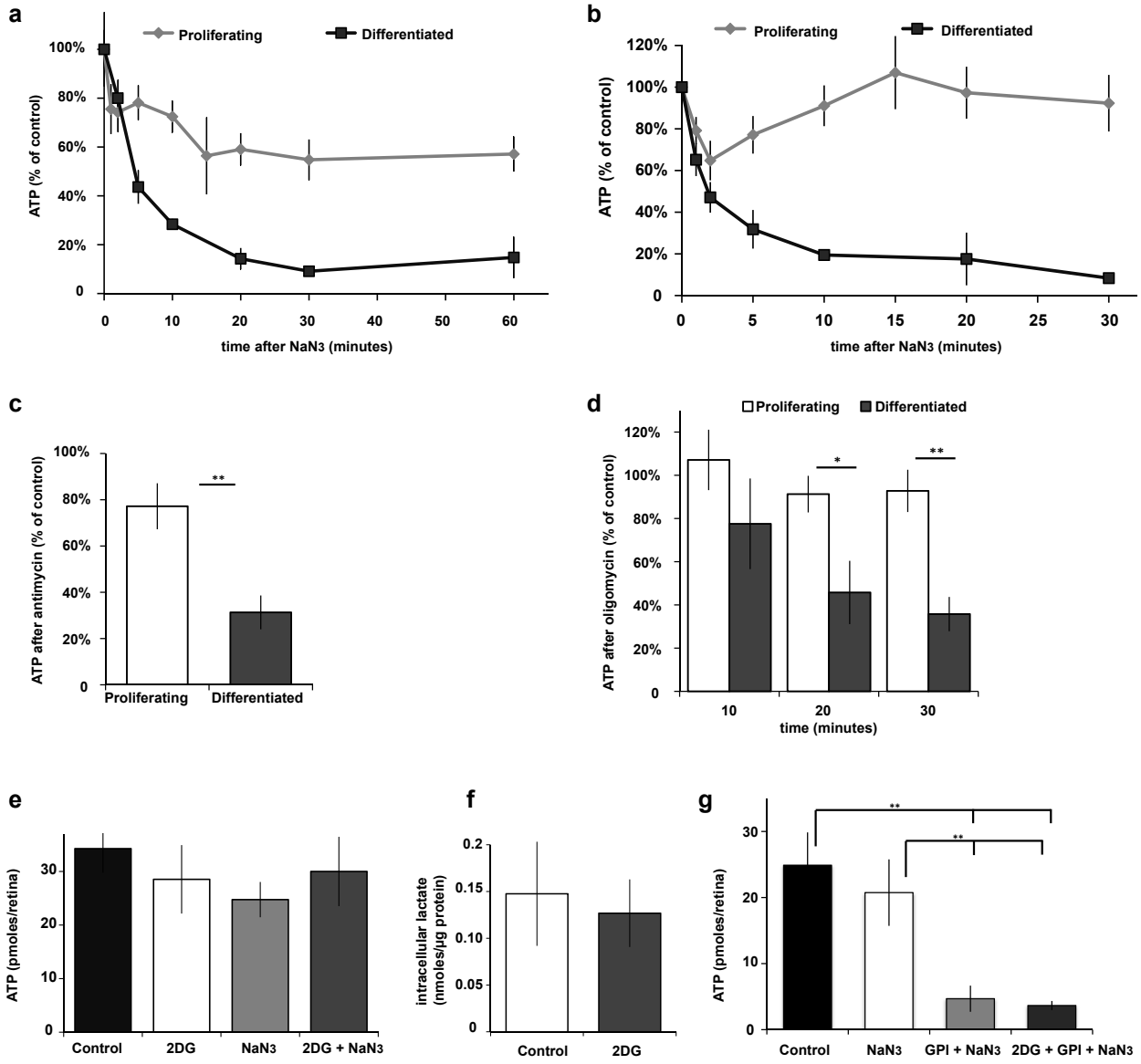

Figure S1 Changes in ATP and lactate in proliferating and differentiated retinas after oxidative phosphorylation and glycolysis inhibitors. **(a)** ATP at different time points after NaN3 addition *in vivo*, normalised to control levels (P, n=4-25 per time point; D, n=4). **(b)** ATP at different time points after NaN3 addition in explants in MBS, normalised to control levels (P, n=4-16 per time point; D, n=4). **(c)** ATP normalised to control levels in freshly dissected explants in MBS with Antimycin A (P, n=13, p=0.003; D, n=13, p=10-6 compared to control; p=4x10-6 drop in proliferating compared to differentiated cells). **(d)** ATP normalised to controls in freshly dissected explants in MBS with Oligomycin (t=10: P, n=5, p>0.05; D, n=5, p>0.05 compared to controls. t=20: P, n=10, p>0.05; D, n=9, p=0.002 compared to controls, and p=0.002 drop in proliferating compared to differentiated cells. t=30: P, n=12, p>0.05; D, n=14, p=2x10-6 compared to controls, p=10-6 drop in proliferating compared to differentiated cells). **(e)** ATP levels in freshly explanted retinas incubated with 2-deoxy-D-glucose (2DG) and NaN3 in 1x MBS (p>0.05 for all conditions, control n=21, 2DG n=8, NaN3 n=5, 2DG + NaN3 n=8). **(f)** Intracellular lactate after 3 hours of incubation with 2DG (n=6, p>0.05). **(g)** ATP levels in freshly explanted retinas in L15, incubated with NaN3, GPI and 2DG (n=5, p<0.001 for GPI + NaN3 or 2DG + GPI + NaN3 compared to control or NaN3 alone). Error bars in all figures show 95% confidence intervals; * 0.001 < p < 0.05; ** p < 0.001.

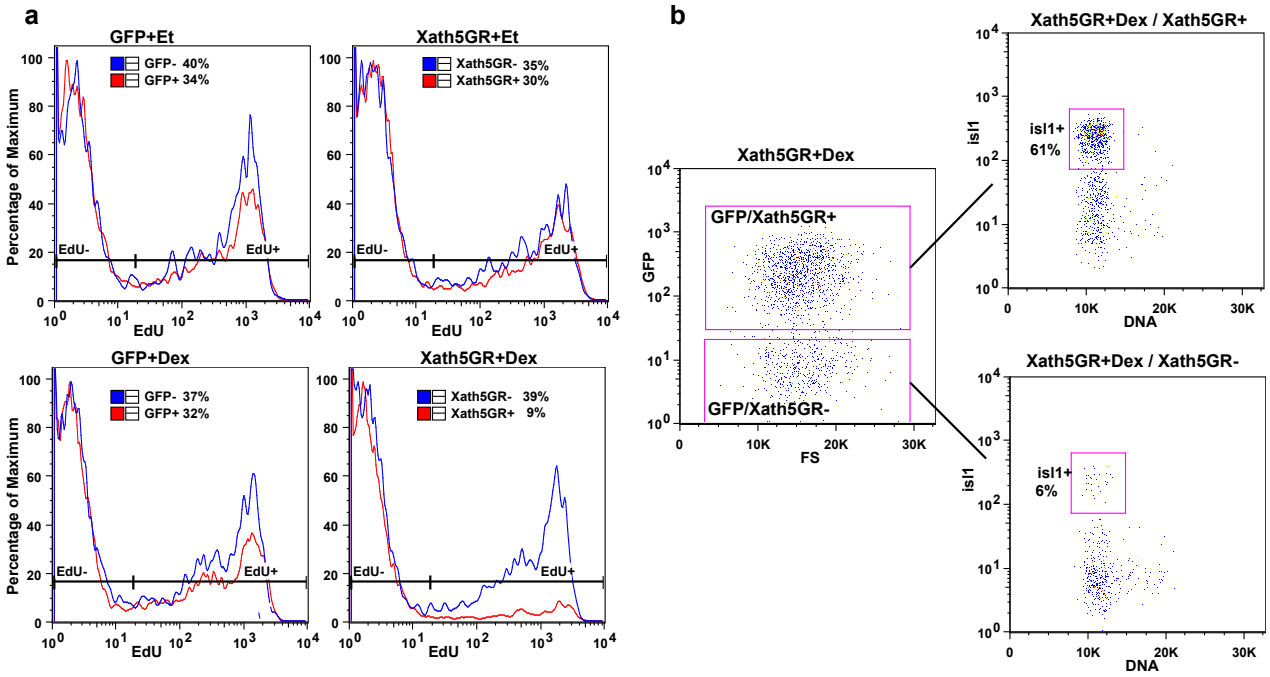

Figure S2 Overexpression of Xath5GR mRNA and induction by dexamethasone (Dex) at stage 25 inhibits proliferation and promotes differentiation into isl1+ cells. **(a)** At stage 33/4, Xath5GR (bottom right panel) inhibits proliferation of overexpressing cells (Xath5GR+, red histogram) compared to non-overexpressing cells in the same retinas (Xath5GR-, blue histogram) when Dex is added, but not when a corresponding concentration of the ethanol (Et) solvent is used instead of Dex (top right panel), or when only GFP mRNA is injected, with or without Dex (left panels). **(b)** GFP/Xath5GR+ cells (top right panel) have a much higher proportion of postmitotic isl1+ cells compared to GFP/Xath5GR- control cells (bottom right) in the same retina at stage 39. The scheme of separation of GFP+ and GFP- cells from the GFP/Xath5GR co-injection is shown on the left panel.

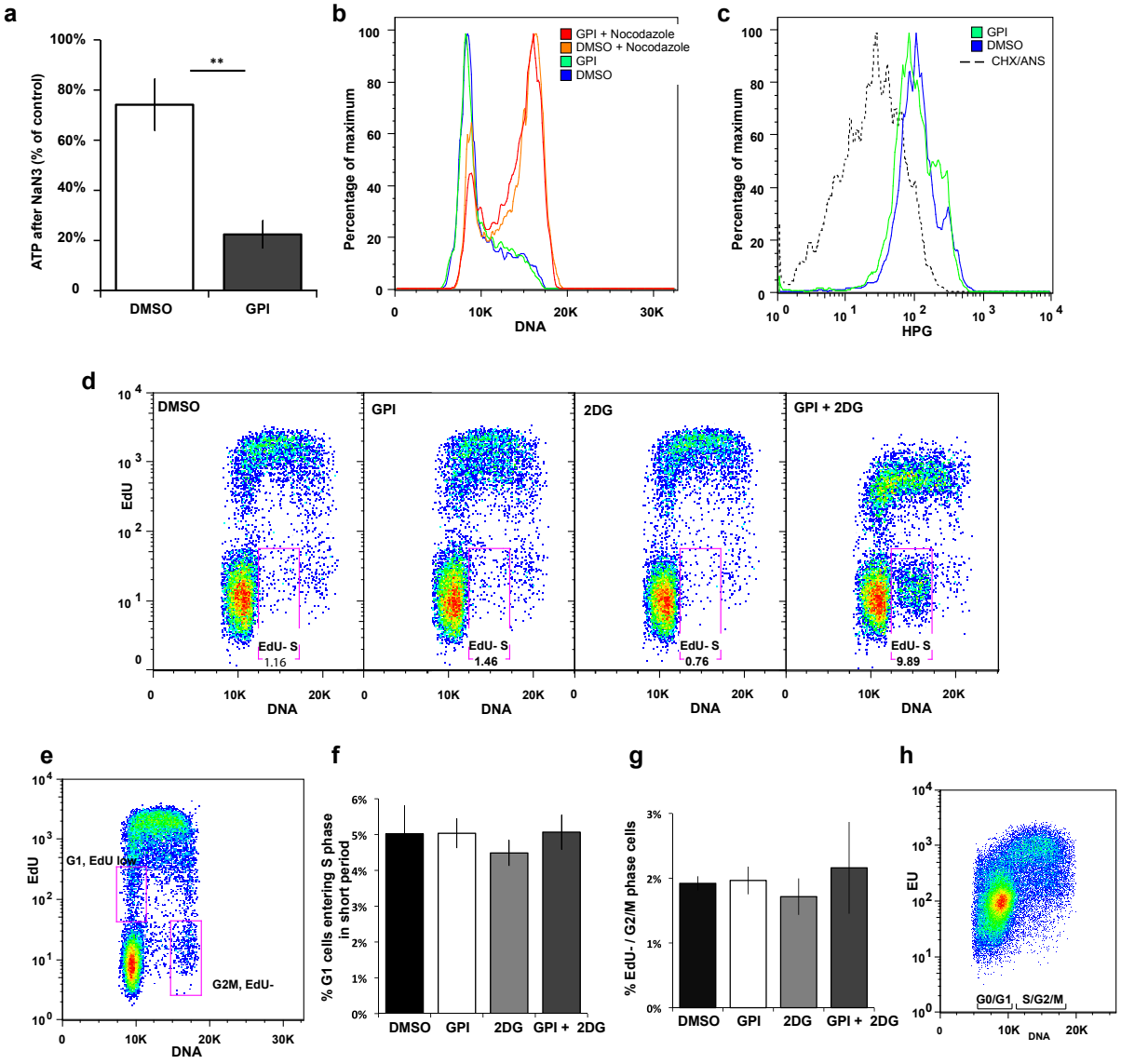

Figure S3 Effects of GPI and 2DG on progenitor cell proliferation. **(a)** Retinal explants incubated with GPI in 1x MBS for 4-7 hours still require oxidative phosphorylation for their ATP (DMSO and GPI, n=15, p=10-7 for difference between DMSO and GPI). **(b)** Incubation of explants with GPI for 4-6 hours does not impede progression of cells through G1 and S phase and accumulation in G2/M during nocodazole block (GPI had no effect compared to control DMSO treatment in 4/4 experiments). **(c)** Incubation of explants with GPI for 8-10 hours does not change the rate of the methionine analogue HPG incorporation into protein. The dashed histogram shows the background levels of fluorescence when the protein synthesis inhibitors cycloheximide + anisomycin are used with HPG. Quantification is shown in Fig. 5j. **(d)** GPI + 2DG reduces or abolishes EdU incorporation in S phase cells (EdU negative/S phase cells shown in box), unlike either drug alone or controls. **(e)** Estimation of G1 and G2/M phase rates after a short (1-2 hour) EdU pulse: 'G1/EdU low' box includes cells that just entered S phase from G1 prior to fixation, therefore the proportion of these cells compared to all G1 cells is an indication of G1 length (a longer G1 should result in a smaller proportion). 'G2M/EdU-' box includes cells that have been in G2/M for the duration of the EdU pulse, therefore the higher the proportion, the longer G2/M should be. **(f)** No effect of GPI and/or 2DG on proportion of G1/EdU low : G1 cells, an indication of G1 rate (n=4). **(g)** No effect of GPI and/or 2DG on proportion of G2M/EdU negative cells, an indication of G2M rate (n=4). **(h)** At stage 25, EU incorporation in explants is higher in S/G2M phase cells compared to G1.

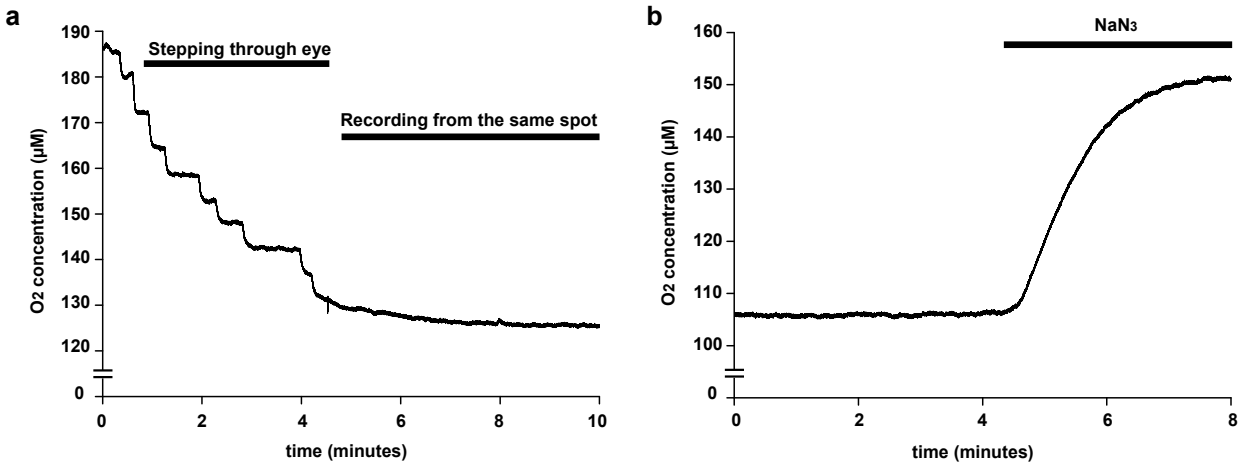

Figure S4 (a) Variation in [O2] as the electrode is pushed deeper in the retina in steps. **(b)** Increase in [O2] deep in the tissue after addition of NaN3 in the bath.

Supplementary Movie Legend

EB3-GFP motion stops in progenitor cells **(a)** earlier than in post-mitotic neurons **(b)**. Embryos were incubated in Antimycin A, and after an incubation period of 20 minutes, imaged by spinning disk confocal microscopy at 20-second intervals. The two examples shown were from the same imaging session and drug treatment in the same dish.